An Analysis of Electric Fields Developed Inside Microchannels of Microfluidic Devices

Bashir I. Morshed
Department of Electronics
Carleton University
Ottawa, ON K1S5B6, Canada

Maitham Shams
Department of Electronics
Carleton University
Ottawa, ON K1S5B6, Canada

Tofy Mussivand
Professor of Surgery and Engineering
University of Ottawa Heart Institute
Ottawa, ON K1Y4W7, Canada

***Abstract*—An analysis of electric fields inside microchannels of microfluidic (MF) devices is reported in this paper. Microchannel-based MF devices using electric fields are of recent research interest for various purposes, including on-chip manipulation of biological elements (cell, DNA, proteins and other macromolecules). To determine electric field strengths inside the microchannels of such devices, the uniform electric field equation (eg. $E = \delta V/\delta l$) is commonly used. However, this can lead to a significant estimation error, especially for smaller dimensions of the microchannel, which is the future trend. Finite element method (FEM) analysis should be performed for such smaller dimensions. However, this method is time consuming and computationally expensive, particularly during design phases, as there exist many unbound parameters. In this paper, analytical expressions to determine electric fields and other parameters of interest are developed for a simplistic model, and then compared the FEM simulation results to that of MF devices for a range of microchannel dimensions. The results show that significant estimation errors can occur. For example, more than 10% overestimation of electric field results in microchannel lengths smaller than 2.5 mm. The analysis and graphs can aid MF device designers during design phases.**

I. Introduction

Microfluidic (MF) devices, such as the lab-on-a-chip (LOC), the micro-total-analysis-system (μTAS), the biomedical microelectromechanical systems (bioMEMS) etc., use microchannels, among other micro-structures, to process biological elements like cells, deoxyribonucleic acid (DNA), proteins, etc. [1]. A commonly used microchannel structure in such devices to develop electric fields inside these microchannels constitutes of excitation voltage applied through electrodes inserted inside reservoirs on both ends of the microchannels [2]–[7]. Applications of such electric field-based microchannels are electrophoresis separation of DNA and proteins, electric field-based cell lysis, drug delivery through electroporation, electro-osmotic flow etc.

Although the electric field inside the microchannel can be described using the *Poisson equation* [1], this is rarely used in practice because it is difficult to apply for any specific MF device. To determine electric field strengths inside microchannels, finite element method (FEM) analysis is sometimes used [5], [8]. FEM analysis, however, is not suitable for the design phase, as the design parameters are sometimes unbound. A few attempts were made to develop analytical expressions to calculate electric fields. Exact expressions were developed for certain MF devices, but these are complex and design specific [8]–[10]. The uniform electric field equation (eg. $E = \delta V/\delta l$) is most commonly used to estimate the electric field strengths [2]–[6]. However, this might result in significant estimation errors, especially for smaller dimensions of microchannel - which is the future trend - as demonstrated in this work.

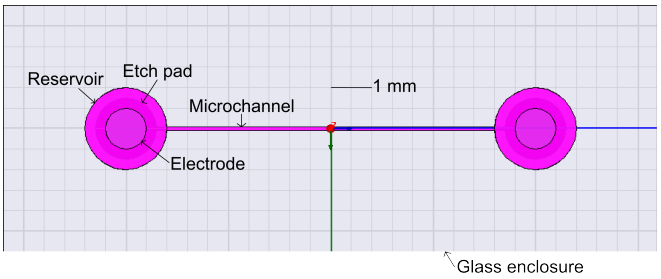

Fig. 1: Top view of a section of the MF device showing a microchannel to be analyzed for developed electric fields.

II. The Microfluidic Device to be Analyzed

The MF device to be analyzed was fabricated using the Protolyne Fabrication Process (Micralyne Inc., Edmonton, Alberta). This foundry allows researchers to obtain the semi-custom MF device fabricated within a short amount of time while being relatively inexpensive. The device consists of two glass-slides, fused together. Eight predefined access holes (i.e. reservoirs) of 2 mm diameter are through-drilled in the top slide. Eight etch-pads of 1.5 mm diameter are etched on the top surface of the bottom slide aligned with the reservoirs. To form microchannels, trenches are etched on the top surface of the bottom slide according to the designer's requirements. These trenches form microchannels when both glass slides are fused together. The length of a microchannel is defined by the intersections of a trench (forming microchannel) and the reservoirs at the ends, while the etch depth is set to 20 μm. Most microfluidic devices share the same topology as this MF device to be analyzed [2], [3], [5], [6].

Fig. 1 shows a section of the design of a microchannel of the MF device joining two access holes (reservoirs). During experiments to develop an electric field inside the microchannel, electrodes are inserted inside these reservoirs. The electric field inside the microchannel is developed by filling

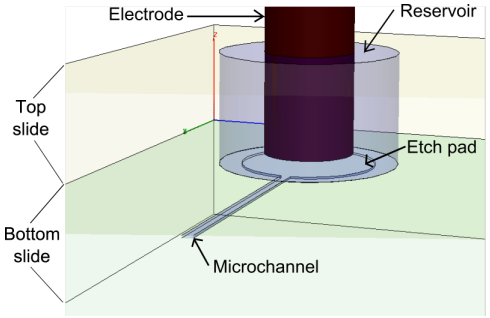

Fig. 2: A 3-D view of a portion of the microchannel of the MF device is shown schematically. The top and bottom glass-slides that compose the glass enclosure are indicated.

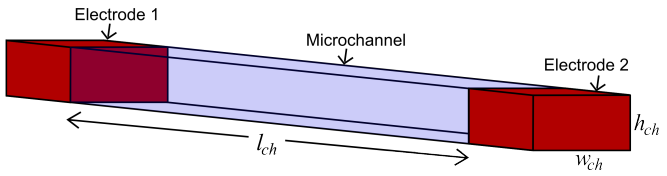

Fig. 3: A simplistic model of a rectangular box shaped microchannel filled with buffer fluid having electrodes on both sides. The whole structure is enclosed within a glass substrate.

the microchannel and the reservoirs with an ionic buffer fluid, such as Dulbeccos Phosphate Buffered Saline (D-PBS), and exciting the electrodes with an applied voltage. This setup is depicted in Fig. 2 using a 3-D view drawing of a portion of the microchannel.

III. Simplistic Model of the Microchannel

To begin electric field analysis of the MF device, a simplistic model of a microchannel structure is considered as shown in Fig. 3. In this simplistic model, the microchannel is a rectangular box with length, width and height of l_{ch}, w_{ch} and h_{ch}, respectively. Both electrodes contact the complete cross-sectional areas on both ends of the microchannel. The microchannel is assumed to be filled with D-PBS buffer fluid, with relative permittivity (ϵ_r) and conductivity (σ_{ch}) of 80 and 1.6 Ω/m, respectively [5]. The whole structure is enclosed within a glass substrate, whose conductivity and permittivity are negligible when compared to those of D-PBS. An electric field, E_{ch}, is developed inside the microchannel as an excitation voltage, V_{app}, is applied across the electrodes. The voltage across the microchannel, V_{ch}, is the same as V_{app} for this simplistic model.

IV. Analytical Expressions for the Simplistic Model

For the simplistic model of the microchannel (Fig. 3), electric flux inside the microchannel can be assumed to be uniform. Thus, E_{ch} can be expressed using the uniform electric field expression between two parallel electrodes [11], as

$$E_{ch} = \frac{V_{ch}}{l_{ch}}. \tag{1}$$

Due to the current flow through the buffer fluid, the (ohmic) power dissipation, P_d, inside the microchannel can be expressed as [12],

$$P_d = \frac{V_{ch}^2}{R_{ch}} \tag{2}$$

where R_{ch} is the electrical resistance of the microchannel. Using the resistivity law [12], R_{ch} for the rectangular box can be expressed as

$$R_{ch} = \rho_{ch} l_{ch} / A_{ch} \tag{3}$$

where ρ_{ch} ($= 1/\sigma_{ch}$) is the resistivity of the buffer fluid inside the microchannel and A_{ch} ($= w_{ch} \times h_{ch}$) is the cross-sectional area of the microchannel. So, from expression (2),

$$P_d = \frac{V_{ch}^2}{\rho_{ch}} \left(\frac{A_{ch}}{l_{ch}}\right) = \frac{E_{ch}^2}{\rho_{ch}} \mathbf{V}_{ch} \tag{4}$$

where $\mathbf{V}_{ch}$ ($= A_{ch} \times l_{ch}$) is the volume of the microchannel. Hence, for a given electric field, the power dissipation is proportional to the volume of the microchannel.

Again, the energy density, u_{ch}, stored inside the microchannel due to the electric field can be expressed by [11],

$$u_{ch} = \frac{1}{2} \epsilon E_{ch}^2 = \frac{\epsilon}{2} \frac{V_{ch}^2}{l_{ch}^2}. \tag{5}$$

Here ϵ ($= \epsilon_0 \epsilon_r$) is the permittivity of the buffer fluid, where ϵ_0 is the permittivity of the free space and ϵ_r is the relative permittivity of the buffer fluid. The total energy stored, U_{ch}, within the microchannel can be obtained by integrating u_{ch} over $\mathbf{V}_{ch}$ [11]. For the rectangular box, U_{ch} can be expressed by the simple expression,

$$U_{ch} = \int_{\mathbf{V}_{ch}} u_{ch} d\mathbf{V} = \frac{1}{2} \epsilon E_{ch}^2 \mathbf{V}_{ch} = \frac{\epsilon}{2} V_{ch}^2 \left(\frac{A_{ch}}{l_{ch}}\right). \tag{6}$$

Again, for a given electric field, the total energy stored is proportional to the volume of the microchannel. From expressions (6) and (4), U_{ch} is proportional to P_d with a proportionality constant of $\epsilon \rho_{ch}$/2.

These analytical expressions (1,4-6) for the simplistic model are plotted in Fig. 4 to 7 (as solid lines) for a range of V_{app}. In Fig. 4 and 6, plots of electric field strengths and energy densities are plotted against the lengths of the microchannels (l_{ch}) using expressions (1) and (5), respectively. Fig. 5 represents power dissipation curves against the area-over-length ratio (A_{ch}/l_{ch}) using expression (4). Fig. 7 shows the relationship of the total energy stored inside the microchannel against A_{ch}/l_{ch} using expression (6).

V. FEM Simulation of the Simplistic Model

The simplistic microchannel model (Fig. 3) was simulated by using an FEM analysis tool (Maxwell3D simulator from Ansoft Corp). A script file was written to simulate 175 different sets of dimensions (l_{ch}, w_{ch} and h_{ch}). The range of l_{ch}, w_{ch} and h_{ch} simulated were 100 to 10000 μm, 1 to 1000 μm, and 10 to 1000 μm, respectively. Each structure was simulated for excitation voltages ranging from 1 V to 1000 V. The material property for the buffer fluid inside

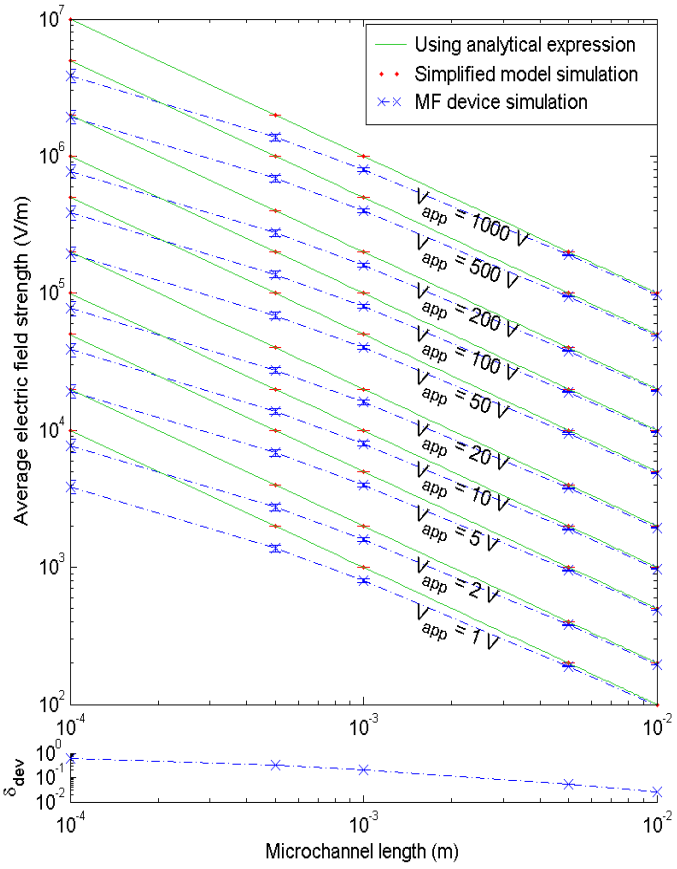

Fig. 4: Plot representing relationship between the developed electric field strengths (E_{ch}) with the lengths of the microchannels (l_{ch}) for various excitation voltages (V_{app}). Normalized deviations (δ_{dev}) are plotted at the bottom. All simulation results include error bars representing standard errors.

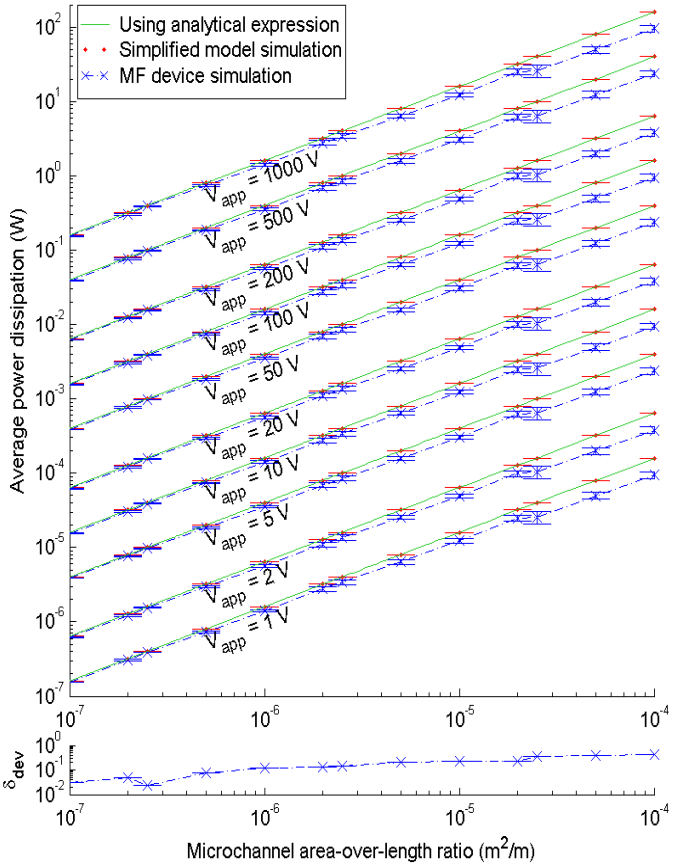

Fig. 5: Plot depicting power dissipations (P_d) for various area-over-length ratios (A_{ch}/l_{ch}) of the microchannels for various excitation voltages (V_{app}). Here, ρ_{ch} = 0.625 Ω-m. Normalized deviations (δ_{dev}) are plotted at the bottom. All simulation results include error bars representing standard errors.

the microchannel was set similar to D-PBS ($\epsilon_r = 80$ and $\sigma_{ch} = 1.6\Omega$/m). The number of iterations was set to 20, as higher iterations provide insignificant change. The resultant data were collected, analyzed, and plotted using Matlab in Fig. 4 to 7. The mean of these data are represented by dots (.), and the standard errors are denoted by the error-bars on both sides of the mean.

These simulation results very closely relate to the analytical expressions. The maximum values of the normalized standard errors are tabulated in Table I. The normalized standard errors are calculated by dividing the standard errors by the corresponding means. The very small values of these normalized standard errors indicate good agreement of the analytical expressions with the FEM simulations.

VI. FEM Simulation of the Microfluidic Device

The MF device model (Fig. 1 and 2) was simulated using another script file with the same FEM analysis tool. Dimensions of the microchannel were varied (exact same ranges as the simplistic model), while the dimensions of the reservoirs, electrodes, and etch holes were kept constant. The electrodes of a 1 mm diameter were positioned in the centers of the reservoirs, 0.1 mm above the bottom plate. The microchannel and reservoirs were assumed to be filled with the same material having properties similar to D-PBS, and the same numbers of iterations were performed. The resultant data were collected, analyzed, and plotted using Matlab and are shown in Fig. 4 to 7. The mean of the data are denoted by crosses ($\times$), and the standard errors are denoted by the error-bars on both sides of the means. The mean values are connected with dot-dashed lines.

The maximum values of the normalized standard errors for this MF device (Table I) are higher compared to those of the simplistic model. These maximum values of the normalized standard errors were below 0.3. This indicates that the y-axis parameters are influenced by additional parameters other than the x-axis parameters. For example, E_{ch} of the MF device is dependent on other parameters (such as w_{ch}, h_{ch} etc.) in addition to l_{ch}.

The mean data of the MF device simulation results deviate from those of the simplistic model, especially for small l_{ch} (i.e. large A_{ch}/l_{ch}). This type of deviation should be taken under consideration for electric field related applications, especially

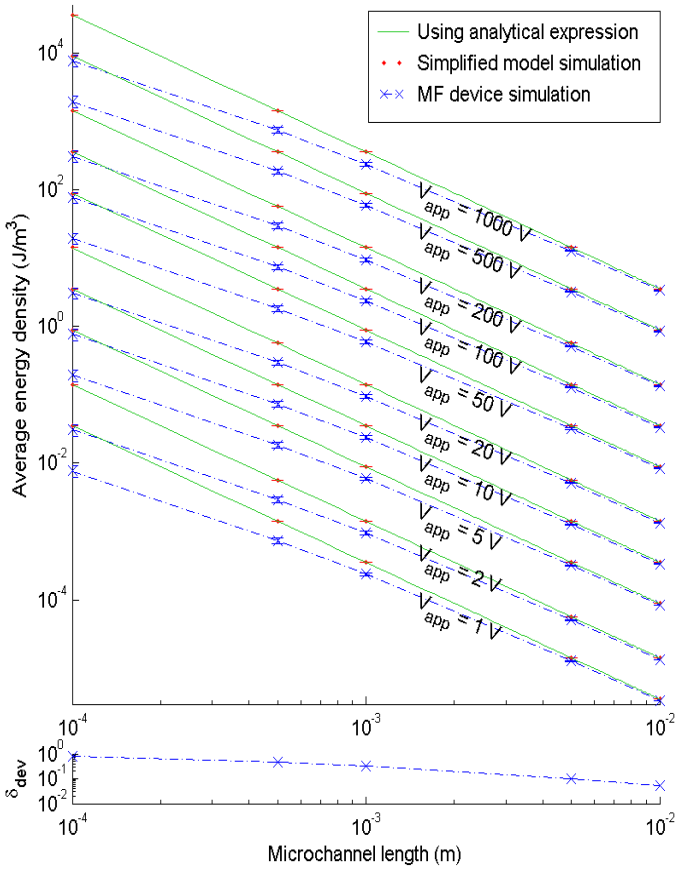

Fig. 6: Plot showing dependance of the energy densities (u_{ch}) inside the microchannels with the microchannel lengths (l_{ch}) for various excitation voltages (V_{app}). Here, ϵ_r = 80. Normalized deviations (δ_{dev}) are shown at the bottom. All simulation results include error bars representing standard errors.

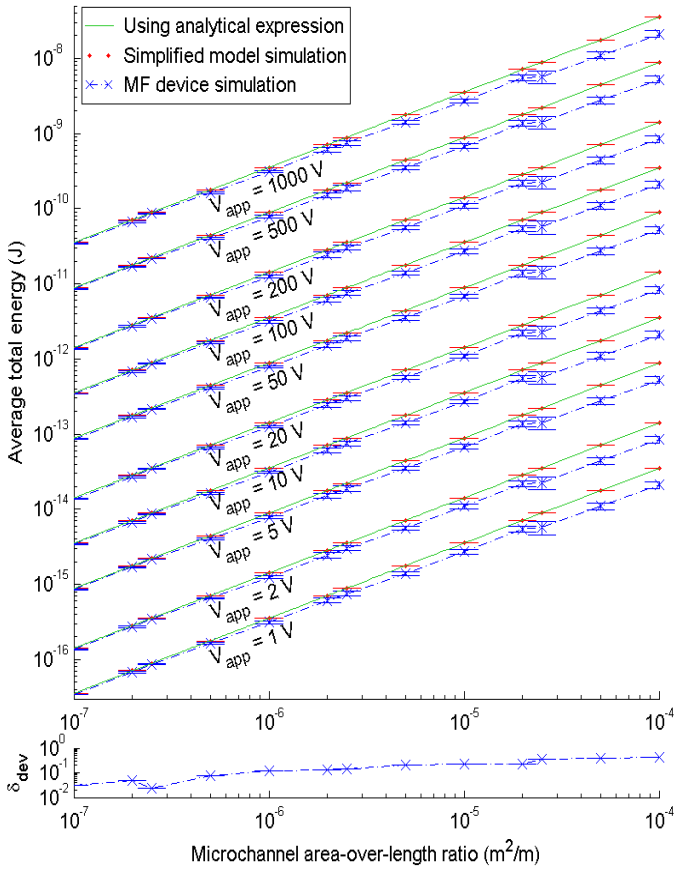

Fig. 7: Plot representing the total energies (U_{ch}) stored versus area-over-length ratios (A_{ch}/l_{ch}) of the microchannels for various excitation voltages (V_{app}). Here, ϵ_r = 80. Normalized deviations (δ_{dev}) are given at the bottom. All simulation results include error bars representing standard errors.

TABLE I: Maximum values of the normalized standard errors from FEM simulations

Plot	**Simplistic model**	**MF device**
E_{ch} vs l_{ch}	0	0.1145
P_d vs A_{ch}/l_{ch}	9.8×10^{-17}	0.2997
u_{ch} vs l_{ch}	1.7×10^{-7}	0.1905
U_{ch} vs A_{ch}/l_{ch}	5.65×10^{-7}	0.2997

TABLE II: Overestimation ranges of the analytical expressions when compared to the MF device simulation results

Parameter	**10% overestimation**	**50% overestimation**
E_{ch}	$l_{ch} < 2.5$ mm	$l_{ch} < 0.1$ mm
P_d	$\frac{A_{ch}}{l_{ch}} > 7\times10^{-7}$ m^2/m	$\frac{A_{ch}}{l_{ch}} > 1\times10^{-4}$ m^2/m
u_{ch}	$l_{ch} < 5$ mm	$l_{ch} < 0.4$ mm
U_{ch}	$\frac{A_{ch}}{l_{ch}} > 7\times10^{-7}$ m^2/m	$\frac{A_{ch}}{l_{ch}} > 1\times10^{-4}$ m^2/m

for the case of small lengths of microchannels [3]–[5]. To quantify these deviations, the normalized deviations (δ_{dev}) are plotted beneath each plots (Fig. 4 to 7). Here, δ_{dev} are calculated by subtracting the mean data for the MF device from the mean data for the simplistic model, then dividing by the mean data for the simplistic model. These plots are averaged for various V_{app}. The mean values of these averages are shown using crosses ($\times$), while the standard deviations are shown as the error bars in these δ_{dev} plots.

The values of δ_{dev} are always positive, indicating the analytical expressions always overestimate, due to the fact that V_{ch} is always smaller than V_{app} in MF devices. As microchannel lengths become smaller (i.e. area-over-length ratios become greater), δ_{dev} values increase. The amount of overestimation can be determined from the δ_{dev} plots. The range for 10% and 50% overestimation are tabulated in Table II. One can rationalize that these estimation errors resulted from the presence of the reservoirs in the MF device. These estimation errors can be minimized by determining V_{ch} for the MF device. To calculate V_{ch}, one has to determine the resistance introduced by the reservoirs, which is tedious, and dependent on the structure and dimensions of the reservoirs.

VII. Conclusions

To analyze the electric fields developed inside the microchannels of MF devices, analytical expressions were developed using a simplistic model. FEM simulations of this simplistic model and the MF device revealed that significant errors are introduced if the analytical expressions for the simplistic model are employed for microchannels of MF devices with very small dimensions. This analysis and the resulting graphs can aid in designing microchannels for developing electric fields, especially during the design phases. Further analysis is being conducted to develop empirical expressions for MF devices by extending analytical expressions for the simplistic model to calculate various parameters of the MF device to achieve a higher degree of accuracy.

Acknowledgement

The authors gratefully acknowledge the contributions of Canadian Microelectronics Corporation (CMC), Natural Sciences and Engineering Research Council (NSERC) of Canada, and Ottawa Heart Institute (OHI).

References

[1] Steven S. Saliterman, *Fundamentals of BioMEMS and Medical Microdevices*, Wiley-Interscience, WA, USA, 2006.

[2] J. Gao, X. Yin, and Z. Fang, "Integration of Single Cell Injection, Cell Lysis, Separation and Detection of Intercellular Constituents on a Microfluidic Chip," *Lab Chip*, vol. 4, pp. 47–52, 2004.

[3] H. Wang, A. K. Bhunia, and C. Lu, "A Microfluidic Flow-through Device for High Throughput Electrical Lysis of Bacterial Cells Basaed on Continuous DC Voltage," *Biosensors and Bioelectronics*, vol. 22, pp. 582–588, 2006.

[4] A. S. Bhagat, S. Dasgupta, R. K. Banerjee, and I. Papautsky, "Effects of Microchannel Cross-section and Applied Electric Field on Electroosmotic Mobility," in *Conf Solid-State Sensors, Actuators and Microsystems*, 2007, pp. 1853–1856.

[5] Dong Woo Lee and Young-Ho Cho, "A Continuous Electrical Cell Lysis Device Using a Low DC Voltage for a Cell Transport and Rupture," *Sensors and Actuators*, vol. B 124, pp. 84–89, 2007.

[6] L. A. Legendre, J. M. Bienvenue, M. G. Roper, J. P. Ferrance, and J. P. Landers, "A Simple, Valveless Microfluidic Sample Preparation Device for Extraction and Amplification of DNA from Nanoliter-volume Samples," *Analytical Chemistry*, vol. 78, no. 5, pp. 1444–1451, 2006.

[7] J. W. Hong, H. Hagiwara, T. Fujii, H. Machida, M. Inoue, M. Seki, and I. Endo, "Separation and Collection of a Specified DNA Fragment by Chip-based CE System," in *Micro Total Analysis Systems*, 2001, pp. 113–114.

[8] A. Jenkins, C. P. Chen, S. Spearing, L. A. Monaco, A. Steele, and G. Flores, "Design and Modelling of a Microfluidic Electro-lysis Device With Controlling Plates," in *Int. MEMS Conf.*, 2006, pp. 620–625.

[9] P. Linderholm, U. Seger, and P. Renaud, "Analytical Expression for Electrical Field Between Two Facing Strip Electrodes in Microchannel," *Electronic Letters*, vol. 42, no. 3, pp. 145–146, 2006.

[10] A. N. Chatterjee and N. R. Aluru, "Combined Circuit/Device Modeling and Simulation of Integrated Microfluidic System," *IEEE J MEMS*, vol. 14, no. 1, pp. 81–95, 2005.

[11] Fawwaz T. Ulaby, *Fundamentals of Applied Electromagnetics*, Pearson Prentice Hall, NJ, USA, 2004.

[12] J. W. Nilsson and S. A. Riedel, *Electric Circuits*, Prentice-Hall, NJ, USA, 2000.